Gaussian quadrature for optical design
with non-circular pupils and fields, and broad wavelength ranges

Brian J. Bauman[a*] and Hong Xiao[b]

[a]Livermore National Laboratory, 7000 East Ave., M/S L-210, Livermore, CA 94550;
[b]Department of Mathematics, University of California, Davis, Davis, CA
[*]bauman3@llnl.gov, phone: 925-423-6592

ABSTRACT

Forbes introduced the usage of Gaussian quadratures in optical design for circular pupils and fields, and for a specific visible wavelength band. In this paper, Gaussian quadrature methods of selecting rays in ray-tracing are derived for non-circular pupil shapes, such as obscured and vignetted apertures. In addition, these methods are generalized for square fields, and for integrating performance over arbitrary wavelength bands. Integration over wavelength is aided by the use of a novel chromatic coordinate. These quadratures achieve low calculations with fewer rays (by orders of magnitude) than uniform sampling schemes.

Keywords: Geometric optical design, lens system design, Gaussian Quadrature, Buchdahl chromatic coordinate

1. INTRODUCTION

Efficient numerical ray-tracing made a great step forward with Forbes' paper in 1988[1], which introduced the use of Gaussian quadrature (GQ) in calculating root-mean-square (rms) spot size for an optical design. For example, ray-tracing methods based on Gaussian Quadrature use knowledge about the maximum order of the aberration in choosing an efficient set of rays, which produce results that are numerically equivalent to those obtained through a direct integration across the entire pupil. See Figure 1 for an example of a GQ ray set.

Gaussian quadrature as discussed in Forbes' paper is applicable to filled, circular apertures, and to elliptical apertures with a small change—these are the most commonly encountered cases in optical design. Often, GQ will still work as a merit function when optimizing an optical system with modest obscuration or vignetting. However, certain systems depart significantly from these cases, among which is the Large Synoptic Survey Telescope (LSST)[2]; see figure 2.
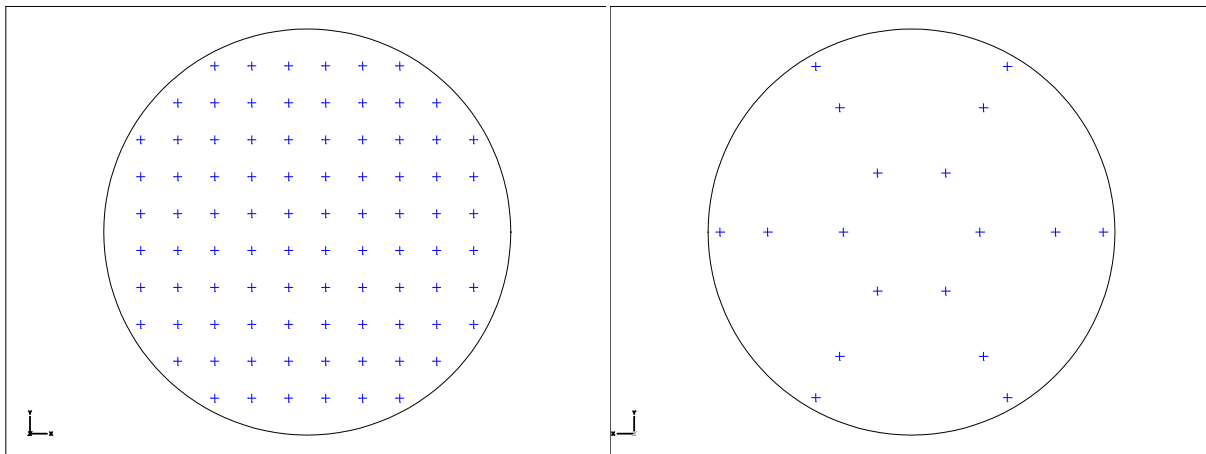

Figure 1: (left) 12x12 uniform grid of rays on a circular pupil; (right) 3-ring, 6-spoke pattern derived from a Gaussian quadrature. The normalized radii are 0.3535, 0.7071, and 0.9420. The GQ ray set has 1/5 as many rays and performs far better.

LSST uses a modified Paul-Baker design, which has 3 mirrors. The primary and tertiary are fabricated out of a single substrate so that they are permanently aligned; this approach was also seen in Rumsey.[3] LSST has a large central

obscuration—about 62% obscuration by diameter. There is also considerable vignetting (of up to 10% by area) when comparing the vignetting at the center of the field versus the edge of the field. These cases are not handled well by the techniques in Forbes's paper. As a result, these cases are often evaluated with large uniform grids of rays, resulting in analysis and optimization that are orders of magnitudes slower than comparable GQ ray sets. In this paper, GQ will be extended to annular as well as vignetted pupils.

Forbes' paper also discusses the application of GQ to the integration of performance parameters across a circular field, and across a wavelength band. However, these applications have been less commonly used. On the other hand, improvement of this kind is available in optimizing most optical designs, and benefits significantly systems such as LSST. Thus, we will discuss these methods in this paper.
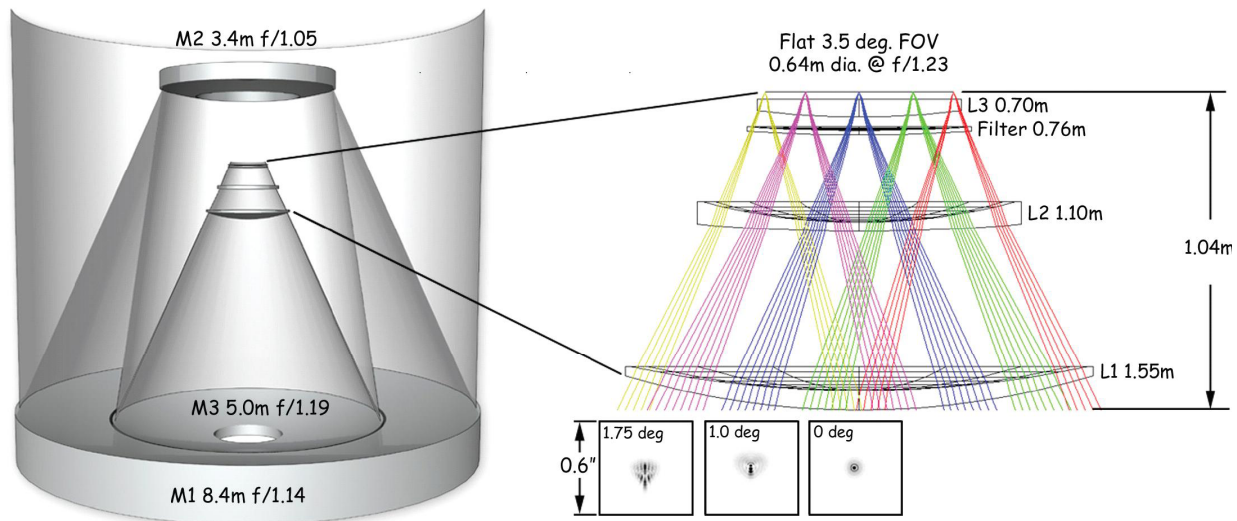

Figure 2: Layout of LSST, with the refractive elements highlighted on the right.

2. GAUSSIAN QUADRATURE ON THE PUPIL

2.1 Gaussian quadrature in one dimension

A quadrature formula is a weighted sum of the values of a function, say $f(x)$, at a relatively small number of points which is equal to the integral I of the function on a certain domain (which is typically chosen to be [-1,1] in one dimension). In other words,

$$I = \int_1^1 \omega(x) f(x) dx = \sum_{i=1}^n w_i f(x_i)$$ (1)

where $f(x)$ is the integrand, $\omega(x)$ is a weight function, x_i are called the nodes, and w_i are called the weights. Typically, quadratures are designed to integrate a pre-selected class of functions accurately, with common choices of functions including polynomials, trigonometric functions, etc. In this paper, we'll use $\omega(x) = 1$ as a common, concrete example.

Gaussian quadratures are a classical formula that is optimal in that in one dimension, an n point Gaussian quadratures can integrate the *2n-1* functions accurately, and no other quadratures can integrate the same functions with *n-1* points. When $\omega(x)$ is uniform and the interval is [-1,1], then the nodes of the n-point Gaussian quadrature are the roots of the n-th Legendre polynomial. For example, a 5th order polynomial can be integrated by evaluating by the 3-point quadrature whose nodes are: $L_i = \left\{ -\sqrt{3/5}, 0, +\sqrt{3/5} \right\}$ with corresponding weights $w_i = \left\{ 5/9, 8/9, 5/9 \right\}$.

In practice, we frequently need to change the integration interval from [-1,1] to [*a*,*b*]. This can be easily accomplished by scaling and shifting.[4] In particular, to convert a tabulated set of sampling points on [-1,1] to an interval [*a*,*b*], we note

that the length of the domain in the first case is 2, and the interval in the second case is *b-a*. Thus, each node should be scaled by a factor of (*b-a*)/2, and then shifted by (*a+b*)/2 to map the center of the [-1,1] interval onto the center of the [*a,b*] interval. Similarly, each weight should be scaled by (*b-a*)/2 in order for the quadrature to integrate correctly the constant on the scaled interval. The corresponding transformations can be written as:

$$L_i' = \left(\frac{a+b}{2}\right) + \left(\frac{b-a}{2}\right)L_i$$
$$w_i' = \left(\frac{b-a}{2}\right)w_i$$

(2)

with L_i, w_i denoting the nodes and weights for the original interval, and L_i', w_i' the nodes and weights for the interval [*a,b*]. The $\left(\frac{b-a}{2}\right)$ factor in the weight equation can also be viewed as the derivative $\frac{du}{dx}$, where $u = \left(\frac{a+b}{2}\right) + \left(\frac{b-a}{2}\right)x$, which is the variable substitution (used in Section 6 below); this derivative is sometimes referred to as a Jacobian. In one dimension, Gaussian quadratures are unique for a given set of functions (not necessarily polynomials).[4] We note that there is an overall scaling factor between weights presented here and those used in commercial lens design codes. For purposes of a merit function, this difference produces no effect since weights are normalized.

2.2 Gaussian quadrature on the circular aperture

As is well known, the aberration functions we are interested in for integration across the aperture are separable in polar coordinates: the radial parameter ρ and the angular parameter θ. A typical basis of these functions are the so-called Zernike polynomials, which are of the form of $R(\rho)\cos(m\theta)$ or $R(\rho)\sin(m\theta)$, where $R(\rho)$ is a polynomial in ρ of degree up to *m*.

We then build a "tensor product quadrature rule" based on the one-dimensional Gaussian quadrature in the radial direction and a uniform sampling quadrature in the angular direction. Since the integrands of interest in the angular direction are of the form $\cos(n\theta)$ and $\sin(n\theta)$ with integer $n \le m$, a maximum of *m+1* evenly sampled angles should suffice.[5] Similarly, a Gaussian quadrature of *k* nodes integrates accurately all monomials up to the (2*k*-1)-th order. Thus, the annular tensor product rule that integrates all Zernike polynomials of degrees up to *m* requires a total of (*m+1*)*(*m+1*)/2 nodes.

For the circular aperture, there are two ways to apply the one dimensional Gaussian quadratures in the tensor product. In reference 1, the Legendre roots L_i are applied to the quantity ρ^2 (which can be thought of as a fractional area *f* integrated from the center of the pupil to a normalized radius ρ), due to the lack of terms involving ρ^{2k+1} for non-negative integer *k*. This transformation of the Gaussian quadrature can be written as,

$$L_i' = \rho_i^2 = \left\{\frac{1+L_i}{2}\right\}$$
$$w_i' = \frac{w_i}{2}$$

(3)

Thus, for a 3-ring case on the circular aperture, the sampled radii and corresponding weights are:

$$\rho_i = \left\{\sqrt{\left(1-\sqrt{3/5}\right)/2} \ \sqrt{1/2}, \ \sqrt{\left(1+\sqrt{3/5}\right)/2}\right\} = \{0.3357, 0.7071, 0.9420\}$$
$$w_i = \{5/9, 8/9, 5/9\}$$

(4)

We note that the weights of the resulting quadrature remain symmetric in the radial direction.

In the second approach, one applies directly the Gaussian quadrature in the radial direction via scaling and shifting of the Legendre roots L_i (see equation (2)). However, in order for the quadrature to be applicable in the polar coordinate, all weights corresponding to nodes in the same ring need to be multiplied by the radius of that ring. The resulting quadrature have sampled radii that are symmetric about the average radius ((1+*a*)/2), and non-symmetric weights in the

same direction. For sampling the disk with 3 rings, the radii of the sampled nodes and the corresponding weights under this method become

$$\rho_i = (1+L_i)/2 = \left\{ \left(1+\sqrt{3/5}\right)\Big/2, \; 1/2, \; \left(1-\sqrt{3/5}\right)\Big/2 \right\} = \{0.1127, 0.5000, 0.8873\}$$

$$w_i = \{0.1127, 0.5000, 0.8873\} * \{5/9, 8/9, 5/9\} = \{0.0626, 0.4444, 0.4929\}$$

(5)

This approach, however, does not take advantage of the lack of odd radial terms in the integrand and so is not as efficient as the method in equation 4.

2.3 Gaussian quadrature on an annular pupil

For the annular case, the sampling radii ρ_i can be found similarly. Suppose that the inner radius of the annulus is a ($0<a<1$), in which case ρ now lives on the interval $[a,1]$, as opposed to $[0,1]$ as in the circular case. The fractional area (cf. section 2.2) still lives on $[0,1]$ and this is the variable to which the Legendre GQ roots will be applied. Thus, the fraction of the area from a to the radius ρ_i to that of the annulus is given by $f_i = \left(\rho_i^2 - a^2\right)\Big/\left(1^2 - a^2\right)$. Therefore, we can find the sampling radii through the equation

$$L_i' = f_i = \frac{\rho_i^2 - a^2}{1^2 - a^2} = \frac{1+L_i}{2} \Rightarrow \rho_i = \sqrt{a^2 + (1+L_i)(1-a^2)/2}$$

(6)

For example, if $a = 0.5$ (or 50% obscuration by diameter), then the sampling radii for the 3-ring case are $\rho_i = \sqrt{a^2 + (1+L_i)(1-a^2)/2} = \sqrt{(5+3L_i)/8} = \{0.5784, 0.7905, 0.9568\}$, with the weights being the same as those for the one-dimensional case: $w_i = \{5/18, 8/18, 5/18\}$.

As in section 3, one can also apply a Gaussian quadrature on the annulus by using scaled-and-shifted Legendre roots L_i as the radii, and then multiplying the weights for each ring by the radius of that ring. Again, the resulting quadrature is symmetric in ring radii about the average radius ($(1+a)/2$), and the corresponding weights are not symmetric:

$$L_i' = \left(\frac{a+1}{2}\right) + \left(\frac{1-a}{2}\right)L_i$$

$$w_i' = \left(\frac{1-a}{2}\right)a \cdot w_i$$

(7)

Figure 3 shows the performance of a quadrature on an annular pupil for LSST vs. a uniform grid. LSST's optics contain 8th order aspheres, which is why several rings are needed. As can be seen, the performance improvement over a uniform grid is similar to that for the circular-aperture case.
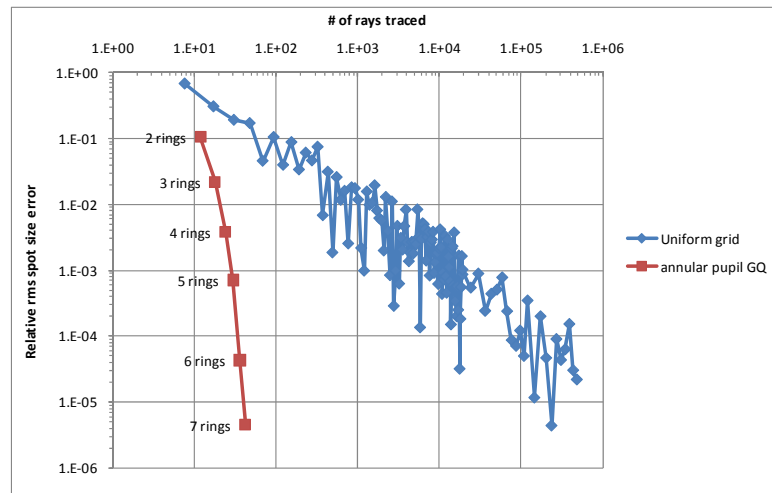

Figure 3: Relative error vs. number of rays traced for LSST annular pupil. To isolate effects due to pupil sampling, rays were traced for a near-axis field and single wavelength only.

2.4 Gaussian quadrature on a vignetted pupil

In many optical designs, vignetting is present where circular or annular pupils are clipped by circular arc(s) along either the inside or the outside edges. We give one example in Figure 4, where the top edge is cut off by an arc of a larger radius. Intuitively, one might expect that a ring-and-spoke pattern can still be used in the vignetted cases. This is, generally speaking, true. Indeed, one can sample along each spoke (radius) following either of the radial sampling methods mentioned in the previous section -- to sample points that are symmetric about the average radius with asymmetric weights, or radii that are not symmetric, but with symmetric weights.

On the other hand, the choice of the angular coordinates can no longer be equally-spaced, if higher ordered sampling is to be achieved. Consider the case in Figure 4 as an example. One certain can break the annulus into two sectors, one on the top that is vignetted, and one at the bottom that is unvignetted. If one chooses to use spokes that are equally-spaced in each sector, the configuration produces an inaccurate formula in the angular direction, since the function $\cos(n\theta)$ and $\sin(n\theta)$ are not periodic in an arbitrarily given angular range. In fact, the convergence of uniform spaced angular sampling points is of order one, leading to the requirement of hundreds of spokes for an accuracy of 2-3 digits.

Fortunately, the difficulty associated with the integration of functions such as $\cos(n\theta)$ and $\sin(n\theta)$ --- which are oscillatory but have limited frequency content --- can be avoided by an alternative approach based on the Prolate Spheroidal Wave Functions (PSWFs).[6] In particular, using an appropriately chosen family of PSWFs, one can construct a quadrature rule that integrate all $\cos(n\theta)$'s and $\sin(n\theta)$'s accurately on the given sector for all n up to m. We list below several examples of these quadratures. Scaling quadratures based on PSWFs the same way as they were the classical Gaussian quadratures, we are able to construct tensor product rules (see Figure 4) that achieve an accuracy of four digits with seven spokes per sector, or eight digits with 18 spokes per sector, as opposed to thousands of nodes required by the uniform sampling scheme. In Appendix A, we summarize a few relevant facts of PSWFs and provide tables of the associated quadratures.
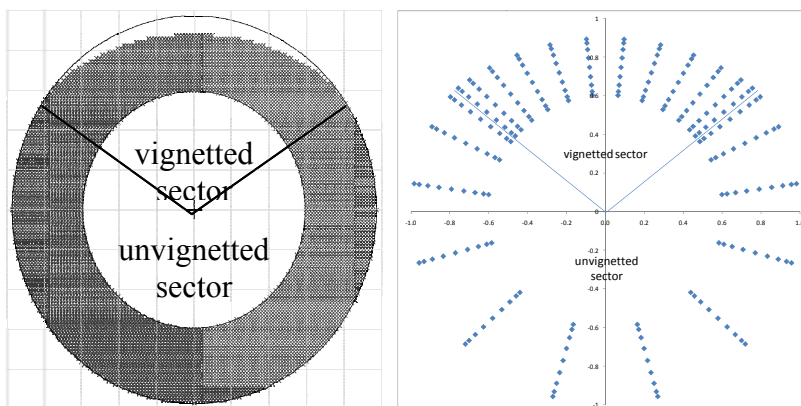

Figure 4: (left) Footprint of the unvignetted light at an LSST-like pupil. Note the large obscuration and vignetting at the top edge. (right) Pattern of sampling points used in GQ calculation to accurately model up to 13th order (much higher than necessary for LSST). Note that there are two sets of spokes: one set for the vignetted section, and one set for the unvignetted section, each with 7 radial points and 8 spokes.

3. GAUSSIAN QUADRATURE IN WAVELENGTH

As discussed by Forbes, GQ in wavelength is inherently much harder than for the pupil or field because the wavelength sampling/weights needs to simultaneously accommodate the several glass types in the lens or in the catalog if optimizing glass selection (although one could assemble a dynamic scheme which adjusts the wavelength sampling according to exactly what glasses are in the lens at the time—it is not obvious that this kind of scheme could be made to work reliably). Fortunately for the lens designer (and unfortunately for the system designer), a figure of merit in wavelength is more elusive and application-dependent, so the goal is often more in the nature of creating a merit function rather than an accurate measure of performance.

GQ can be applied to sample the wavelength band. Because the refractive index of glasses is poorly fitted by a polynomial in wavelength, Forbes suggested substituting the wavelength with the Buchdahl chromatic coordinate
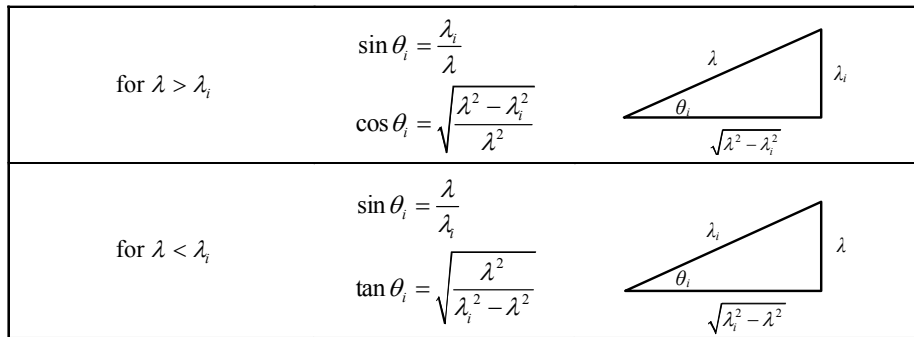
$$\omega = \frac{\lambda - \lambda_0}{1 + \alpha(\lambda - \lambda_0)} \tag{8}$$

and applying GQ to the Buchdahl chromatic coordinate. This produces a better fit, but only over a fairly limited range. Buchdahl[7] and Forbes found that with $\lambda_0 = 0.589\mu$, $\alpha = 2.5$ worked reasonably well for $\lambda = 0.4\text{-}0.7\mu$, but Chipman[8] found that $\alpha = 1.5$ worked better for $\lambda = 0.7\text{-}0.9\mu$ (note that the selection of λ_0 is arbitrary). Robb used $\alpha = 2.5$, but added more terms to extend to about 1μ.[9] The lack of generality in these results suggests that a different variable substitution is called for. Further, a more flexible method would be useful so that designers can more easily set up a variable substitution that is more appropriate for their specific application.

Perhaps the most commonly-used formula for the refractive index is the Sellmeier equation, which is based on a theory of resonances:[10]

$$n^2 - 1 = \sum_i A_i \frac{\lambda^2}{\lambda^2 - \lambda_i^2} \tag{9}$$

where each term represents the effect of an absorption line: the λ_i's represent the absorption wavelengths and the A_i's represent the strengths of the absorption lines; typically, there are 3 terms. An inspection of this equation indicates that polynomials in λ or $1/\lambda$ are not good fits for this equation except for a very limited wavelength range. Upon further reflection, one sees a trigonometric substitution may be fruitful:

for $\lambda > \lambda_i$	$\sin\theta_i = \dfrac{\lambda_i}{\lambda}$ $\cos\theta_i = \sqrt{\dfrac{\lambda^2 - \lambda_i^2}{\lambda^2}}$	*(right triangle: hypotenuse λ, vertical side λ_i, horizontal side $\sqrt{\lambda^2 - \lambda_i^2}$, angle θ_i)*
for $\lambda < \lambda_i$	$\sin\theta_i = \dfrac{\lambda}{\lambda_i}$ $\tan\theta_i = \sqrt{\dfrac{\lambda^2}{\lambda_i^2 - \lambda^2}}$	*(right triangle: hypotenuse λ_i, vertical side λ, horizontal side $\sqrt{\lambda_i^2 - \lambda^2}$, angle θ_i)*

Using j to refer to absorption lines blueward of the desired wavelength range, and k to refer to absorption lines redward of the desired wavelength range, the Sellmeier equation can be rewritten as:

$$n^2 - 1 = \sum_j \frac{A_j}{\cos^2\theta_j} + \sum_k A_k \tan^2\theta_k$$

$$\text{where} \quad \begin{cases} \sin\theta_j = \dfrac{\lambda_j}{\lambda} \\ \sin\theta_k = \dfrac{\lambda}{\lambda_k} \end{cases} \tag{10}$$

The angles θ_i are not angles in any physical sense—they merely allow the use of the aforementioned PWSF GQ constructs for trigonometric functions. For a typical glass, the 3-term Sellmeier equation uses $\lambda_i \approx 0.1\mu$, 0.2μ, 10μ. For a range of $\lambda = 0.4\text{-}0.7\mu$, the corresponding "angles" ranges are 0.14-0.25, 0.28-0.5, and 0.04-0.07 radians. With some additional algebra, one can express the angles θ_2 and θ_3 in terms of θ_1 and derive an expression for index with low orders of trigonometric functions of θ_1. The point is not to derive that expression, but to show that the θ_1 substitution makes sense, because making that substitution allows us to avail ourselves of known methods of GQ for trigonometric integrands, as shown below. It is perhaps a bit arbitrary that the expression is taken in terms of θ_1 rather than the other angles, but it is justified by the fact that the $\lambda = 0.1\mu$ absorption line usually has the strongest effect on the refractive index in the visible and near-IR bands.

Of course, this is only an expression for the refractive index. We are interested in an rms spot size for the lens, which would involve complicated formulas involving the refractive index, even if we could write it analytically (also, expression is in n^2 not n). As mentioned earlier, it is perhaps not even necessary to calculate the spot size accurately as

long as the calculated quantity can act as a merit function of the lens. The idea is that the proper selection of wavelengths and weights reduces the "toothpaste tube" effect, and this approach is more sensible than a uniform spacing of wavelengths or *ad hoc* fiddling of wavelengths and weights. A more thorough study of the effectiveness of the method is beyond the scope of this introductory paper and is planned for future work.

For the present time, it will suffice to see if this approach predicts average spot size over a wavelength range more efficiently than a uniform sampling of wavelengths for a few sample cases.

As mentioned above, trigonometric integrands are non-trivial for domains which do not span an integral number of periods, and a method for the integration of these functions using prolate spheroidal wavefunctions have been developed.[6] The table in the Appendix shows a table of PWSF quadratures over a domain of [-1,1] (note the quadratures are symmetric about x=0). In order to apply these to our situation, we will need to rescale these coordinates as in equation (2) and as above, the weights will be modified by the Jacobian, i.e.,

$$w_i' = w_i \frac{d\lambda}{d\theta_1} = w_i \frac{\lambda^2}{\lambda_1} \cos\theta_1 \qquad (11)$$

and then normalized, as necessary for the task at hand.

As an example, we can generate a 4-wavelength quadrature with a wavelength range of [0.4,0.7μ] and λ=0.1μ. Flipping the wavelength range for convenience, the range of θ_1 is then $\left[\arcsin\left(\frac{0.1\mu}{0.7\mu}\right), \arcsin\left(\frac{0.1\mu}{0.4\mu}\right)\right]$, which is [0.1433,0.2527] in radians. This is now the domain [a,b] that [-1,1] is mapped onto via equation 2. The θ's can then be transformed back into wavelengths for use in the optical design code.

The resulting GQ wavelengths and weights are given in Table 2, alongside the values from Forbes' paper, showing very good agreement. Note that the wavelength nodes are clustered towards the blue end of the spectrum and are more sparse at the red end. This is generally true when using GQ on wavelength and makes sense because the index changes more rapidly towards the blue end, requiring a denser set of nodes there to maintain control of the performance.

Table 2: 4-point quadrature for λ=0.4μ-0.7μ using the techniques in this paper. L_i and w_i are the "raw" nodes and weights from the table in the Appendix. L'_i and w'_i are after the variable substitution to θ. The final nodes and weights to be used are in the shaded columns. Forbes' values for the same case are also given; the results are very similar. Note that the weighting is normalized so that the sum of the weights equals the wavelength range (0.3); this is to allow comparison to Forbes' table.

L_i	$L'_i=\theta_i$	λ_i	λ_i (Forbes)
-0.845401980	0.24423	0.41355μ	0.410836μ
-0.321309809	0.21558	0.46748μ	0.460136μ
0.321309809	0.18045	0.55719μ	0.554033μ
0.845401980	0.15180	0.66130μ	0.662979μ

w_i	w_i'	w_i' (Forbes)
0.375765873	0.03409	0.028202
0.624160603	0.072855	0.071776
0.624160603	0.104232	0.112203
0.375765873	0.088818	0.087820

The difference here, though, is that the present method can be used over a broader and user-selected wavelength range, rather than just the specific ranges covered in the literature. To illustrate, we consider 3 variations of a F2/KzFSN5/FK51 f/10 triplet, with each version optimized mildly for 3 different wavelength intervals: 0.4-1.5 microns, 0.4-1.8 microns, 0.4-2.2 microns. A typical rms spot size vs. wavelength curve is illustrated in figure 5, showing a number of oscillations in performance over the wavelength range. It is this curve that we wish to integrate in a root-mean-square sense.

For wavelengths longer than about 1.5μ, the effect of the infrared absorption line starts becoming significant: there is often an inflection in the dispersion curve around 1.5-1.8μ. The simple substitution using λ_1=0.1μ becomes less effective, and either more wavelength nodes or a slightly different variable substitution is called for.

Currently, we have implemented this approach only for typical glasses such as those found in the Schott or Ohara catalogs. The approach works because all these glasses are very similar in that they have their principal absorption at around 0.1μ. We have not yet tried the technique with other media, such as infrared materials, or with catalogs of more dissimilar materials. This is clearly an area of future effort.
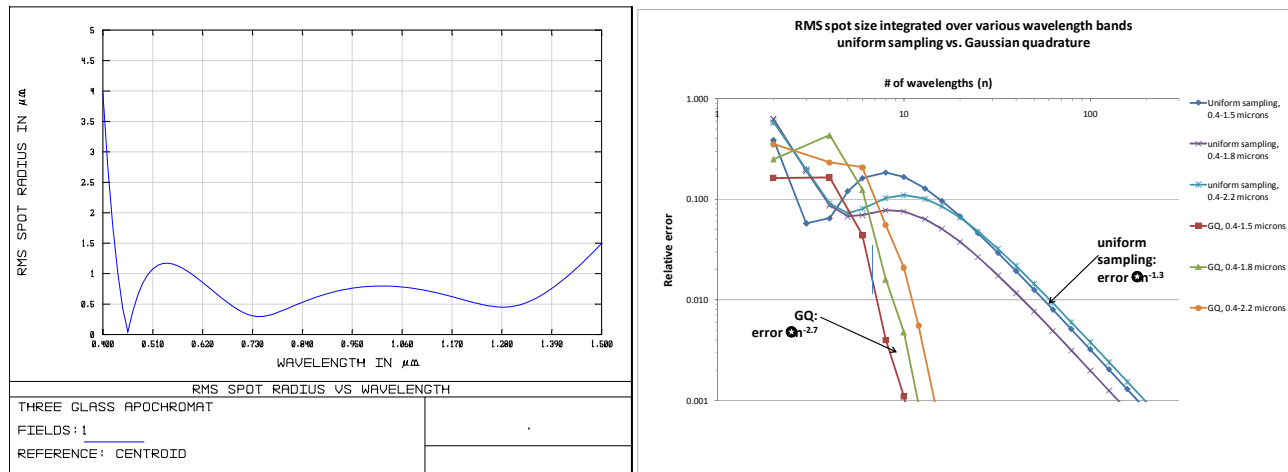

Figure 5: (left) rms spot size versus wavelength over a range of 0.4-1.5μ; note the high order of the wavelength dependency, as evidenced by the number of oscillations; (right) shows that this simple Gaussian quadrature scheme in wavelength produces results that are orders of magnitude more accurate than that produce by uniform sampling of wavelength. Comparing the three GQ curves, we see that as bands go further into the infrared, the convergence becomes slower. This is due to the effect of the infrared absorption line, which becomes increasingly important. However, the method still works remarkably well.

4. GAUSSIAN QUADRATURE ON THE FIELD

4.1 GQ on a circular field

Forbes applies GQ to integrating performance across a circular field. Mathematically, this is identical to the notion of integrating across a circular pupil, and so GQ works in exactly the same way. The field-dependence of the rms spot size is not always of the same order as the pupil-dependence, and it can be higher-order or lower-order than the pupil dependence. For LSST, the orders are about the same. The relevant merit function (MF) is the rms spot size, averaged across the field where every field point is equally important, and this is well-suited to Legendre-based GQ. Forbes discusses a common scenario where the performance is more important in the center of the field and he describes a fourth-order weighting. There is no fundamental difference in these two cases—GQ still applies and only the sampling points and their weights change.

4.2 GQ on a rectangular field

For a rectangular field with uniform weighting, an efficient Gaussian-like quadrature is available.[11] Figure 5 shows the field points for a square field for a 10-point and a 16-point sampling scheme. The precise field values and weights are shown in Table 4. The 10-point scheme is appropriate for a system whose field dependence is described by a 6th order polynomial and the 16-point scheme is appropriate for a system whose field dependence is described by a 8th order polynomial. LSST is used as an example, except with a square field assumed; figure 6 shows the rms spot size vs. field position, and some of the high-order field dependence is evident (arising from the 8th-order aspheres). Figure 6 shows that the performance of a 16-point Gaussian quadrature scheme is equal to a uniform field sample with 1000 times as many field points.
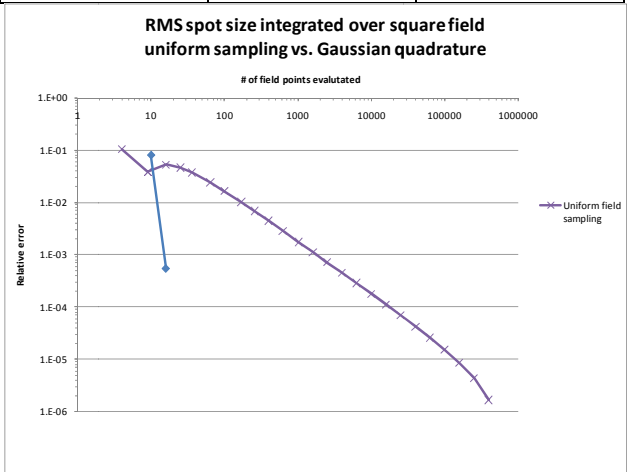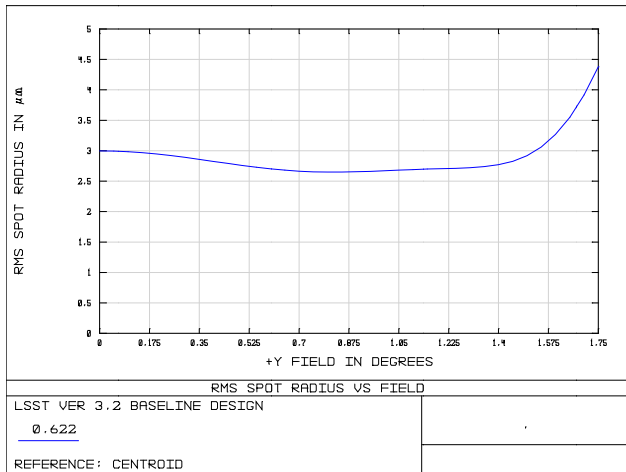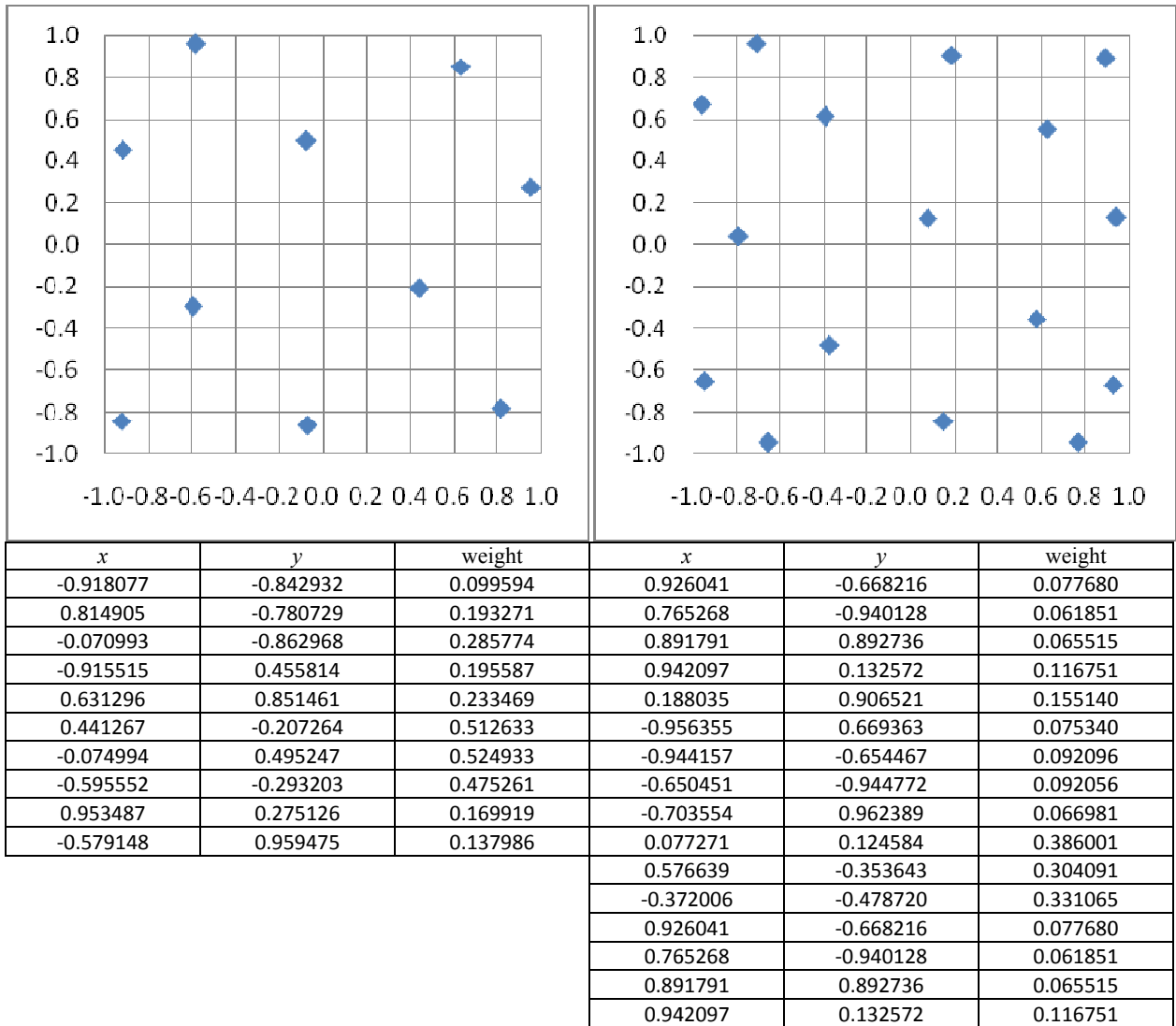
x	y	weight
-0.918077	-0.842932	0.099594
0.814905	-0.780729	0.193271
-0.070993	-0.862968	0.285774
-0.915515	0.455814	0.195587
0.631296	0.851461	0.233469
0.441267	-0.207264	0.512633
-0.074994	0.495247	0.524933
-0.595552	-0.293203	0.475261
0.953487	0.275126	0.169919
-0.579148	0.959475	0.137986

x	y	weight
0.926041	-0.668216	0.077680
0.765268	-0.940128	0.061851
0.891791	0.892736	0.065515
0.942097	0.132572	0.116751
0.188035	0.906521	0.155140
-0.956355	0.669363	0.075340
-0.944157	-0.654467	0.092096
-0.650451	-0.944772	0.092056
-0.703554	0.962389	0.066981
0.077271	0.124584	0.386001
0.576639	-0.353643	0.304091
-0.372006	-0.478720	0.331065
0.926041	-0.668216	0.077680
0.765268	-0.940128	0.061851
0.891791	0.892736	0.065515
0.942097	0.132572	0.116751

Figure 6: 10-point quadrature (top left) and 16-point quadrature (top right) for a square field using normalized coordinates; the precise values are given in the tables in the middle row; (bottom left) rms spot size vs. field; (bottom right) comparison of rms spot size across field using uniform field grid spacing vs. GQ spacing.

CONCLUSIONS AND FUTURE WORK

We have demonstrated extensions to Forbes' Gaussian Quadrature theory for annular and vignetted pupils, for square fields. In addition, we have used a new chromatic coordinate transformation that allows GQ to be applied over large and user-selectable wavelength ranges. In all cases, the performance of these GQ methods is orders of magnitude better than uniform sampling techniques, as we have come to expect from GQ.

Future work will include easy-to-implement GQ for arbitrary pupil and field shapes, and with different weightings. Currently, it is known how to do GQ for polygonal areas, but these are not necessarily easy to implement for optical designers. In addition, it would be useful to have GQ for other curved-boundary pupil shapes. In GQ over wavelength bands, there is much work ahead to assess the effectiveness of this method over a variety of design conditions, and to extend the method to include infrared glasses and other materials that are not similar to standard glasses, Further, effort will be required to evaluate the effectiveness of the approaches to wavelengths where the infrared absorption line is significantly impacting performance.

APPENDIX: PROLATE SPHEROIDAL WAVE FUNCTIONS

Prolate Spheroidal Wave Functions is a class of special functions that are solutions to a certain second order ordinary differential equations. They are also eigenfunctions of the Fourier integral operator on a finite interval: corresponding to the maximum eigenvalue of the sinc operator:

$$\lambda \psi(t) = \frac{1}{\pi} \int_{-T/2}^{T/2} \frac{\sin 2\pi W(t-s)}{t-s} \psi(s)\, \mathrm{d}s \qquad (12)$$

For each positive value of $c = \pi WT$, there is a corresponding family of real-valued, band-limited functions that $\{\psi_m^c\}_{m=0}^{\infty}$ satisfy the integral equation (14), and $\{\psi_m^c\}_{m=0}^{\infty}$ possess a number of mathematical properties, of which the most interesting to our applications is that they form a basis for all functions that have finite integrals on the interval, say [-1, 1]. Denoting the Fourier transform of the m-th function ψ_m by Ψ_m, we summarize the relevant properties as follows. The reader is referred to reference 4 for more details.

P0: ψ_m's are infinitely differentiable on the entire real line.

P1: $\{\psi_m^c\}_{m=0}^{\infty}$ are orthonormal and complete in $\boldsymbol{L}^2[-T/2, T/2]$: $\int_{-T/2}^{T/2} \psi_m(t)\psi_n(t)\, \mathrm{d}t = \delta_{mn}$, where δ_{mn} is the Kronecker delta.

P2: Ψ_m are orthogonal and complete in $\boldsymbol{L}^2[-W, W]$: $\int_{-W}^{W} \Psi_m(f)\Psi_n(f)\, \mathrm{d}f = \lambda_m \delta_{mn}$. Thus the energy of Ψ_m in $[-W, W]$ is λ_m.

P3: ψ_m is even when m is even and is odd when m is odd.

P4: Among functions in $\boldsymbol{L}^2[-T/2, T/2]$, the highest possible energy concentration of their Fourier transforms in $[-W, W]$ is λ_0, and is achieved by Ψ_0.

P5: For each positive integer n, the Fourier transform of ψ_N achieves the highest energy concentration in $[-W, W]$ among all functions in $\boldsymbol{L}^2[-T/2, T/2]$ that are orthogonal to the linear space spanned by $\{\psi_0, \dots, \psi_{n-1}\}$. In addition, the energy concentration decays exponentially as n increases for all n sufficiently large.

Due to P5 and the orthogonality of the first m PSWFs, we can show that a quadrature with nodes being the roots of ψ_m's can integrate all functions in the linear space spanned $\{\psi_0,\ldots,\psi_{n-1}\}$. In addition, with the proper selection of c, the band-width parameter of the PSWFs, the quadrature integrates all functions in $\boldsymbol{L}^2[-T/2, T/2]$ on $[-W, W]$ to an accuracy of $O(\lambda_{m+1})$.[6]

# nodes	x	w	# nodes	x	w	# nodes	x	w
2	±0.548740	1.000000		±0.975160	0.062711		±0.990452	0.024131
4	±0.845402	0.375766		±0.877091	0.129518		±0.952560	0.050243
	±0.321310	0.624161	12	±0.723945	0.173273		±0.892796	0.068018
6	±0.921217	0.195692		±0.536367	0.199530		±0.818612	0.079522
	±0.630684	0.366352		±0.328719	0.214196		±0.735062	0.087067
	±0.221711	0.437953		±0.110649	0.220772	24	±0.645288	0.092162
8	±0.955279	0.113001		±0.984206	0.039983		±0.551255	0.095693
	±0.778290	0.233792		±0.921085	0.084077		±0.454251	0.098173
	±0.503061	0.309230		±0.820587	0.114817		±0.355157	0.099909
	±0.173384	0.343977	16	±0.695031	0.134825		±0.254617	0.101088
10	±0.966472	0.084406		±0.553324	0.147627		±0.153129	0.101821
	±0.835720	0.171228		±0.401351	0.155671		±0.051101	0.102174
	±0.635361	0.224559		±0.243079	0.160402			
	±0.394673	0.253567		±0.081388	0.162598			
	±0.133622	0.266240						

ACKNOWLEDGMENTS

REFERENCES

[1]] Forbes, G. W., "Optical system assessment for design: numerical ray tracing in the Gaussian pupil," JOSA A 5, 1943-1956 (1988).

[2] Olivier, S.S., L. Seppala, and K. Gilmore, "Optical design of the LSST camera," Proc. SPIE, 7018, 70182G (2008).

[3] J. Ma, V. Rokhlin and S. Wandzura, "Generalized Gaussian Quadrature of Systems of Arbitrary Functions," SIAM Journal of Numerical Analysis 33(3), 971-996 (1996).

[4] N. Rumsey, "A compact three-reflection camera," Proc. Optical Instruments and Techniques, 8, 514-520 (1969).

[5] Burden, R. L. and Faires, J. D., [Numerical Analysis], Thomson Brooks/Cole, Belmont, CA, Chapter 8 (2005).

[6] H. Xiao, V. Rokhlin and N. Yarvin, ``Prolate Spheroidal Wave Functions, Quadrature and Interpolation,'' Inverse Problems 17, 805-838 (2001).

[7] Buchdahl, H., [Optical Aberration Coefficients], Dover, New York, 150-154 (1968).

[8] Chipman R.A. and Reardon, P.J., "Buchdahl's glass dispersion coefficients calculated in the near infrared," Applied Optics 28, 694-8 (1989).

[9] Robb, P.N. and Mercado, R.I., "Calculation of refractive indices using Buchdahl's chromatic coordinate," Applied Optics 22, 1198-1215 (1983).

[10] Born, M. and Wolf, E., [Principles of Optics], Cambridge University Press, Cambridge (1997).

[11] Xiao, H. and Gimbutas, Z., ``A numerical algorithm for the construction of efficient quadrature rules in two and higher dimensions,'' Computers and Mathematics with Applications 59, 663-676 (2010).